

Cracks distance and width in reinforced concrete membranes: experimental results from cyclic loading histories



G. Ruocci⁽¹⁾, C. Rospars^(1,2)

⁽¹⁾Laboratoire 3SR, Université Joseph Fourier – Grenoble 1, Grenoble INP, CNRS UMR 5521
Domaine Universitaire, 38041 Grenoble cedex 9, France

⁽²⁾Université Paris-Est / IFSTTAR, 58 boulevard Lefèbvre, 75015 Paris, France

P. Bisch, S. Erlicher

EGIS Industries, 4 rue Dolores Ibarruri, TSA 50012, 93188 Montreuil cedex, France

G. Moreau

EDF R&D, Département STEP, 6 quai Watier, 78401 Chatou, France

SUMMARY

This paper deals with the analysis of cracking pattern in reinforced concrete membranes subjected to shear cyclic load. The results of an extensive experimental campaign that was carried out in the framework of the French research programme CEOS.fr are here presented. A measuring technique based on digital images correlation is used to evaluate displacement and strain fields. Cracks patterns are characterised in terms of cracks spacing, orientation and average width. A comparison between the evolutions of cracks width for two different types of cyclic loading is presented and discussed. Maximal and residual cracks width at a load level close to the ultimate state are analysed in view of the assessment of industrial structures against severe seismic events. This study aims at enhancing the understanding of cracking phenomena in reinforced concrete structures and at providing a contribution to the updating of engineering design formulas through a consistent experimental validation.

Keywords: shear walls, crack patterns, cyclic loading, image correlation, experimental results.

1. INTRODUCTION

The evaluation of crack spaces and widths is an important aspect of reinforced concrete structures design (Kaufmann and Marti, 1998, Pimentel et al., 2010, Polak and Vecchio, 1993). This kind of information is generally required for checking the structure against the serviceability limit state. Moreover, the evaluation of crack widths is strongly related with durability and sometimes confinement issues, in particular for nuclear power plants. For practical applications, the calculation of cracks spacing and widths must be based on standards like, among others, the Model Code (CEB-FIP 1990, FIB 2010) and Eurocode 2 (CEN 2005). However, the formulas provided by these documents are semi-empirical, and mainly developed for beam elements. Their reliability is questionable for thick walls.

Cracking assessment is commonly limited to load cases considered for serviceability requirements. For industrial structures where the tightness should be maintained throughout extreme accidental load cases, it is important to know the state of cracking during and particularly after severe actions, for instance earthquakes. This implies the evaluation of cracking at the Ultimate Limit State (ULS), while existing formulas deal only with the Service Limit State (SLS). Furthermore, experimental data are still missing for validation and/or calibration of models incorporating non-linear constitutive relationships used to derive accurate information about cracking patterns and their variability. In order to assess the accuracy of the standards when their formulas are applied to bi-dimensional reinforced concrete elements until ULS conditions, several experimental tests have been carried out in the framework of the French national research project CEOS.fr (IREX 2008, Rivillon and Gabs, 2011). Both monotonic and cyclic tests have been realized and the crack patterns have been monitored at several load levels. This paper presents a summary of the experimental results, mainly concerning cyclic tests on shear walls, and gives a first comparison with the Eurocode 2 predictions.

2. CEOS.FR PROJECT: SHEAR WALLS MOCK-UPS

The CEOS.fr (« Comportement et Evaluation des Ouvrages Spéciaux – Fissuration, Retrait ») research programme concerns those “special” structures that are not covered by the current engineering practice. The reasons can be due to either their sizes (very massive structures) or unusual in-service requirements (long life-cycle, leak tightness, etc.), or because of special requirements related to the protection against external threats or hazards. In most cases, the design of such structures does not only involve their strengthening capacity, but it also implies the knowledge of the crack pattern under the series of expected situations (Demilecamps et al. 2010).

The general objective of this research project is to make a significant step forward in the engineering capabilities for assessing crack patterns of concrete structures and predicting the expected pattern under given design conditions. This general objective is detailed in three areas, corresponding to different types of physical phenomena to be considered and modelled both experimentally and numerically:

- cracking under monotonic load history;
- thermo-hydro-mechanical behaviour (early-age, shrinkage, creep, long-term drying, etc.);
- seismic and cyclic load histories.

The present paper focuses on the last subject and presents some preliminary results obtained from the test campaign carried out on reinforced concrete walls subjected to in-plane mono and bi-directional cyclic loading histories.

2.1. Shear walls design and instrumentation

The design of the mock-ups aimed at accurately reproduce reinforced thick shear walls used in industrial buildings. Both the selection of materials and the geometry of the specimens were derived from reduced scale modelling issues. As the goal was to evaluate the behaviour of walls beyond the ULS, a 1/3 modelling scale was adopted to adapt the availability of the testing facilities (capacity of the actuators limited to 4,5MN) to these purposes. Geometry scaling factors lower than 1/3 were discarded because of the difficulty of micro-concrete and rebars to reproduce the reference materials grading and ductility, respectively. Therefore, a C40 class concrete was used with bars of 10mm diameter and 100mm spacing in both vertical and horizontal directions on both faces of the wall, in order to test the mock-ups in almost pure shear. Interference between bending and shear cracking modes is prevented by limiting the slenderness of the mock-up. This leads to design the wall with a height/length ratio of $\frac{1}{4}$.

Two horizontal concrete beams with high reinforcement ratio are horizontally connected to the wall to allow a better redistribution of the shear force in the upper and bottom sides of the membrane. Vertical steel bars with 25 and 32mm diameter are used to reinforce the right and the left sides in order to control the crack opening due to bending. Finally, the dimensions of the mock-up are 1,05m of height, 4,2m of length and 0,15m of thickness, which leads to a “full-scale” wall sufficiently thick to be representative of an industrial structure. The reinforcement ratio was selected of about 1%, which is representative of the real situation in such structures. This ratio is also higher than the usual minimum ratio requirement insuring the non-brittleness of the wall and still remaining compatible with the capacity of the jacks. The wall was also designed to obtain a large domain of cracks formation in order to have a clear understanding of the phenomenon.

The testing device was developed to meet the needs of the wall-testing campaign. The bench test is made of two metal structures each of 6,30m x 2,60m set on either side of the wall (see Fig. 1a). The horizontal load is supplied by two 4,5MN capacity hydraulic jacks whose axes are located 100mm from the top of the wall. The horizontal and vertical movements of the test body are respectively prevented by the restraining effect of the frames and a vertical pre-stressing load of 1000kN, both applied at each end of the lower beam through Dywidag bars (see Fig. 1b).

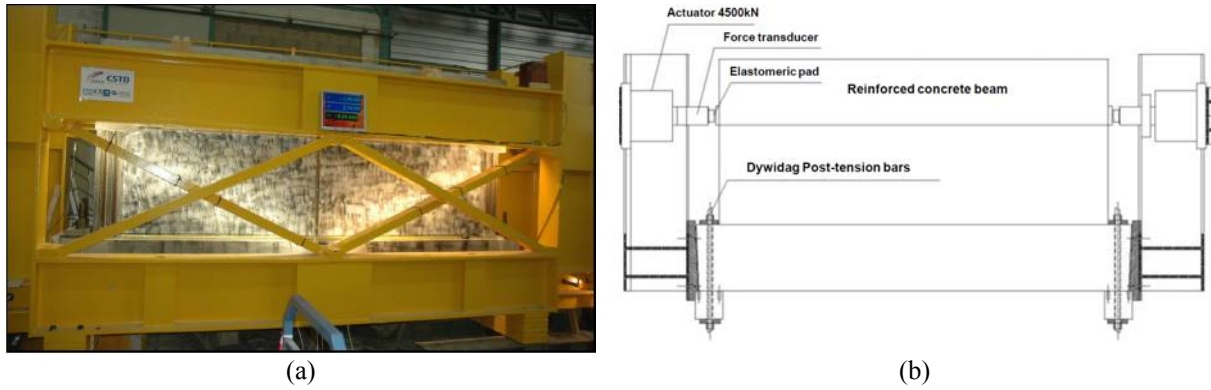


Figure 1. Global view of the steel frame used as “reaction wall” (a) and scheme of the test set-up (b).

Three mock-ups were subjected to horizontal bi-directional cyclic loading that was applied to the top of the wall in series of three cycles with a $\pm 300\text{kN}$ increase between each sequence, until complete failure. A fourth wall was tested to mono-directional cyclic loading (a single push direction), with a single load-unload-reload cycle. The mono-directional and bi-directional cyclic load time histories measured by the force sensors placed at the hydraulic jacks’ location are shown in Fig. 2a and Fig. 2b, respectively. The three walls subjected to bi-directional loading differ only for the type of concrete employed (in one case C25 instead of the default C40) and the reinforcement mesh (in one case 8mm diameter spaced at 8mm instead of the default 10mm at 10mm). For the sake of brevity, only the results for two specimens (the bi-directional cyclic load reference wall and the mono-directional cyclic load wall) are presented in this work. The discussion about the effects of the modification of concrete and reinforcement properties will be deferred to future works.

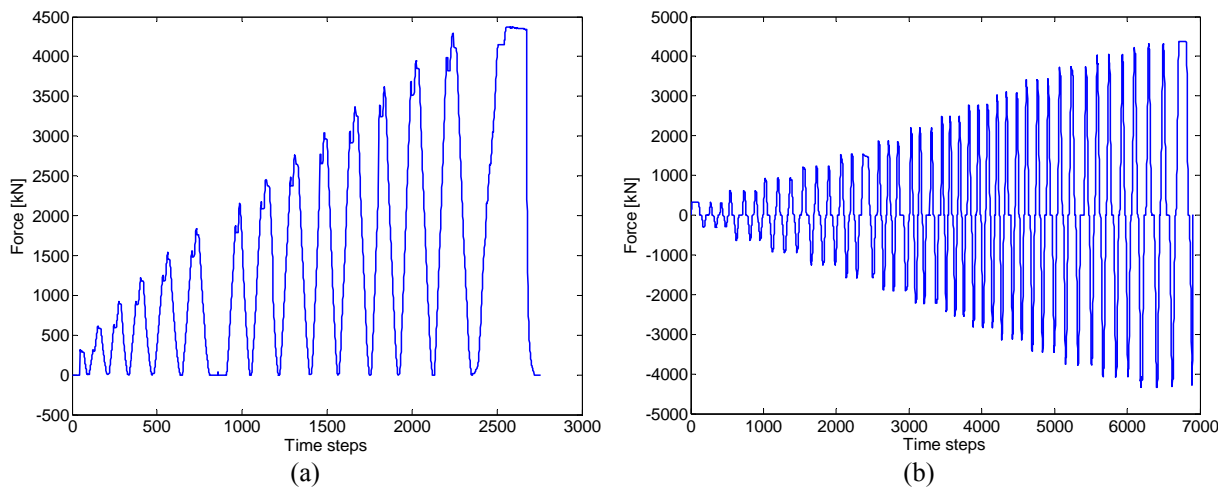


Figure 2. Measured mono-directional (a) and bi-directional (b) cyclic load time histories.

Each testing body was equipped with several sensors that were used to monitor in real-time the state of the test and to assess *a posteriori* the evolution of the cracking pattern. The sensors deployed on the walls count 6 displacement transducers, 17 “long base” optical extensometers set on the whole side of the walls, 19 Bragg fibre optic sensors placed on some spots of the reinforcement bars together with 40 electrical strain gauges. These instruments are able to provide only a punctual or at least “linear” description of the mechanical behaviour of the specimen throughout the test. As the characterisation of the cracking pattern plays a fundamental role within the research project, Digital Image Correlation (DIC) was employed to acquire information concerning the opening of cracks on the whole surface of the test body. The basic principles of this experimental technique are briefly summarised in the following sections and some preliminary results are presented to draw some considerations about the cracking of reinforced concrete structures subjected to shear stress.

2.2. Results of the experimental tests

The horizontal displacements of the mock-ups under the cyclic loading are measured by means of a couple of sensors placed on the upper and lower beams at the boundaries of the wall. The relative displacement is obtained as difference of the measurements of the two sensors. The relationship between the applied force and the relative displacement for the mono-directional and bi-directional cyclic load cases is provided in Fig. 3a and Fig. 3b, respectively. The plot shown in Fig. 3b is obtained by superimposing the response to force F_1 directed towards the left-side of the test body (blue curve) and that obtained for force F_2 in the opposite direction (red line). Both force signatures have been recorded simultaneously during the tests, with one measuring 0 when the load was applied in the opposite direction. This explains the zero force values collected on the axis of abscissas in Fig. 3b. The decrease of the stiffness for increasing load levels is clearly recognizable for both cases from the reduction of the slope of the tangent to the curves. The resistance and ductility expressed respectively by the ultimate force and displacement values are comparable for the two walls. As expected, hysteresis cycles increase throughout the test, which proves the energy dissipation related to cracking phenomena.

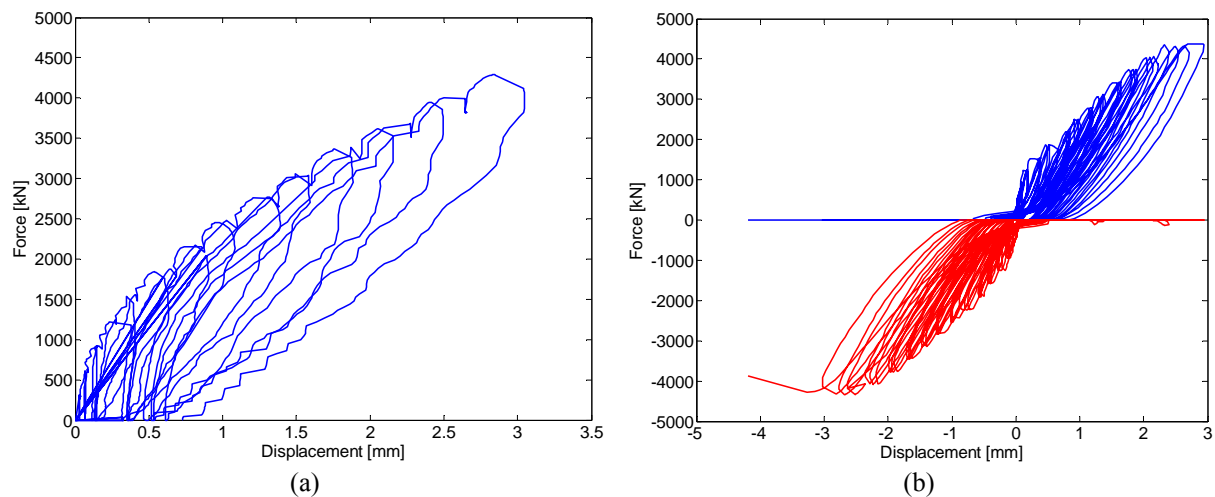


Figure 3. Force-displacement measured for the mono-directional (a) and the bi-directional (b) cyclic load cases.

The occurrence of the first crack was visually noticed at the force level $F_1 = 900$ kN for both walls. The evolution of the crack pattern was qualitatively recorded through visual inspection after each load step. A comparison between the cracks detected for the two walls is presented in Fig. 4. The grids traced on the surface of the walls correspond to the position of the 100mm-spaced reinforcement layers. Obviously, two sets of cracks oriented along symmetrical directions are observed for the bi-directional cyclic load case. The two sets of cracks opened alternatively according to the direction of the applied force. In Fig. 4, cracks represented from top-right to bottom-left appeared for the force pushing towards the left side of the test body (F_1), whereas cracks in the symmetrical direction opened when the load was applied towards the right side (F_2). The opening of some cracks was monitored during the tests by means of extensometers (LVDT) fixed to the wall and crossing a crack at the locations marked in Fig. 4. This instrumentation allowed following the opening (and closing for the bi-directional cyclic load case) of some cracks in a continuous manner. However, the acquired information is referred to a small portion of one crack, which is not representative of the whole cracking pattern. Moreover, the measure is affected by a systematic error since the extensometer is fixed to the wall after the visual detection of the crack, i.e. when this is already opened and is approximately 0,03-0,05mm large. DIC can overcome these drawbacks as it provides an image of the whole crack pattern (although at discrete time steps according to the frequency of images capture) and the measure of the crack width is not affected by systematic errors. In the next paragraph, the basic principles of the displacement field measurement via DIC will be briefly recalled and the methodology adopted to characterize the cracks patterns will be presented in more details.

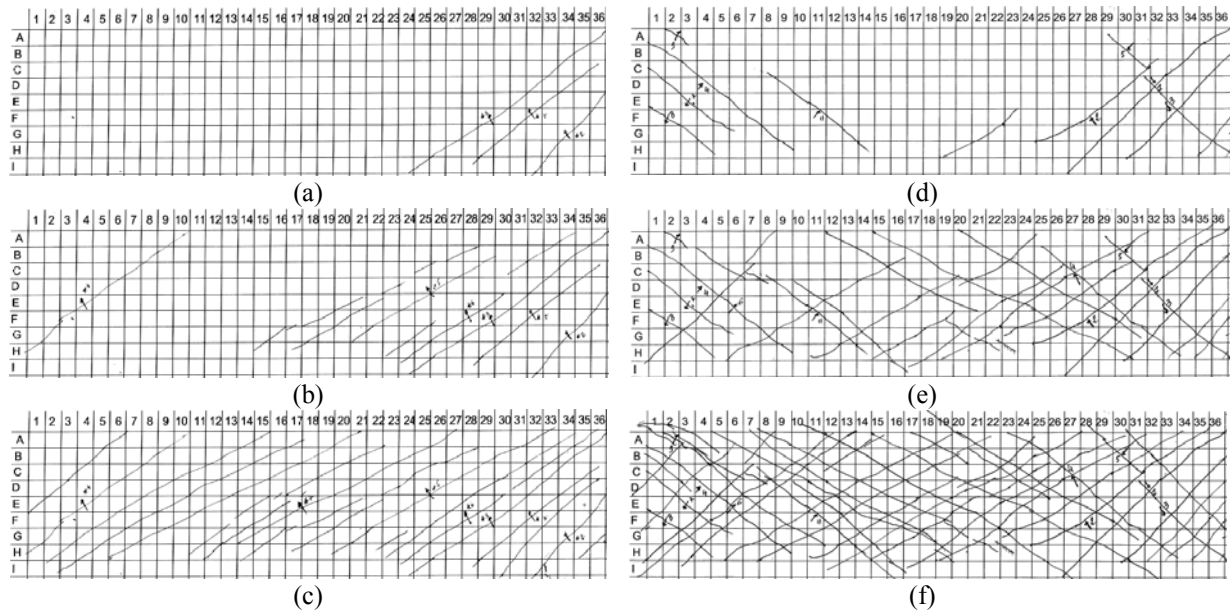


Figure 4. Visually detected crack patterns for the mono-directional cyclic load at 1500kN (a), 2400kN (b), 4200kN (c) and for the bi-directional cyclic load at 1500kN (d), 2400kN (e), 4200kN (f) (Rivillon Gabs 2011).

3. DIGITAL IMAGE CORRELATION: CRACKS DETECTION AND MEASURING

3.1. Basic principles of Digital Image Correlation

Digital Image Correlation (DIC) is an optical technique to measure changes in images in order to analyse 2D and 3D displacement fields. Its early development dates back to '80s (Sutton et al., 1983), but recent technological advances in digital cameras have considerably increased its popularity and widened its application to different areas of science and engineering. Concerning mechanical testing, DIC have been especially applied to measure displacement and strain at the nano and micro-scale due to its contact-free implementation. However, the versatility of the technique allows extending the scale of observation to the macroscopic domain keeping the type of analyses essentially unchanged. In the present study, the selection of the image correlation technique was motivated by the need of characterising the cracking evolution on the widest possible area of the mock-ups.

DIC is based on the maximisation of correlation between the same subset of two images: a “deformed” and a reference image. The displacement field is obtained as that providing the maximum correlation between these two subsets. The correlation can be evaluated either in the reference space or in the Fourier space. Thanks to use of the Fast Fourier Transform (FFT), the second approach is more computationally effective. The quantities that are correlated are the pixel intensities, i.e. the grey scale values, digitized by a digital camera. A bi-quadratic sub-pixel interpolation is then employed to acquire a better precision of the measure, which can attain 0.1pixels. An enhancement to this correlation method has been proposed by Hild et al. (2002) to cope with the analysis of large deformations. A multi-scale correlation algorithm is implemented which consists in forming super-pixels by averaging the grey levels of the pixels contained in each super-pixel. A coarser texture is thus obtained and a first estimation of the displacement is updated by means of an iterative procedure. When convergence is reached the analysis is performed on subsequently finer scales up to the pixel size, i.e. the original images.

3.2. Image acquisition, displacement and strain measurement and cracks analysis

A multi-scale approach to image correlation was applied to analyse the images acquired throughout the cyclic tests carried out on the shear walls in order to deal with the large deformations observed by

contact sensors (LVDTs and strain gauges). For each test, three cameras have been used to cover the whole surface of the wall. The left, central and right view areas captured by the three cameras have been slightly overlapped in order to ensure the continuity of the measured fields. Commercial cameras with 4272x2848 pixels resolution and 12 bits encoding were employed. Since the length of each view measures about 1,5m, the physical size of each pixel is of about 0,53mm. The expected precision of the image correlation is 1/20 of pixel, which corresponds to 26 μ m of measurements precision (Rouzaud, 2011). An example of the left, central and right views acquired by digital cameras is presented in Fig. 5. The surface of the wall was previously treated by projecting black spray paint through pierced plates on the lighter concrete background. The resulting random speckle pattern provides the needed contrast to correlate images accurately. The truss of the steel frame together with all the other portions of image out of investigation was digitally masked to prevent errors that could affect the analysis. As an example, the results of image correlation performed on the wall subjected to mono-directional cyclic load in terms of horizontal displacement and longitudinal strain fields are shown in Fig. 6 and Fig. 7, respectively (Rouzaud, 2011). These results refer to the force level $F_1=3600$ kN, which corresponds to one of the last load steps before failure. At this load level the crack pattern, which can be qualitatively recognized by the change of colour nuance in Fig. 6 and more clearly by the lighter lines in Fig. 7, is completely established (see Fig. 4).



Figure 5. Images of the shear wall surface acquired by the three digital cameras employed in the tests.

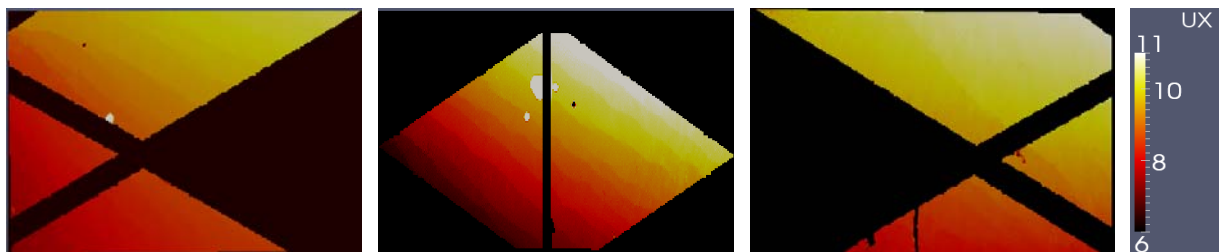


Figure 6. Horizontal displacement fields at $F_1=3600$ kN for the wall tested to mono-directional cyclic load.

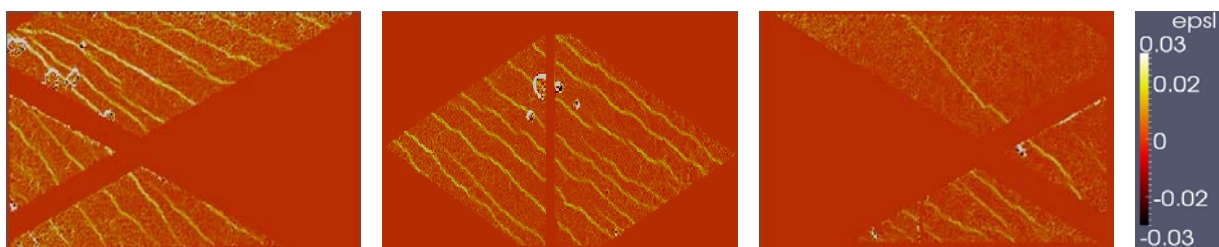


Figure 7. Longitudinal strain fields at $F_1=3600$ kN for the wall tested to mono-directional cyclic load.

A post-processing tool has been developed to automatically analyse the strain fields resulting from DIC and obtain the cracks spaces and widths. For the sake of brevity, in this work we focus only on the results of the central view (see Fig. 5-7) as the shear stress in this portion of the wall is supposed not altered by flexion. The evolution of the shear cracking for both load histories was analysed by defining a reference crack pattern on the basis of the results of the last load steps and then proceeding backwards in the spacing and width measurement of the detected cracks. Each crack was detected by means of a “peak-picking” procedure carried out on the strain field obtained from DIC. This technique

is based on the assumption that cracks correspond to those zones (approximately lines) of the specimen where a discontinuity in the displacement field is observed. In the strain field, these discontinuities appear as peaks. Thus, the strain field is sampled by windowing; for each window mean values and standard deviation are summed in order to define a threshold value. The pixels whose strain value overpasses this threshold are identified as crack points and linking successive crack points together allows tracing a crack line.

The measurement of the crack widths is performed at each crack point as the difference of the displacement fields evaluated at the selected crack location and then projected on the direction orthogonal to the crack line. The reference crack patterns that have been detected for the two shear walls are depicted in Fig. 8 and Fig. 9. In the case of the bi-directional cyclic load the crack patterns are represented separately as they appeared alternately according to the direction of the force applied. It is worthy to stress that the orientation of cracks portrayed in Fig. 8 and Fig. 9 is inverted compared to that of Fig. 4 as images were acquired on the surface of the walls opposite to the face where cracks were visually detected. In both figures, the circles represent the crack points and their diameters provide an indication of the crack opening at each point. The number of detected cracks is 10 for the mono-directional cyclic load and 11 for the bi-directional one. The good correspondence with the records of the visual detection (Fig. 4) in terms of number, location and orientation of cracks proves the symmetry of the cracking mechanisms between the faces of the mock-ups and confirms the accuracy of the tests.

The whole set of identified crack points is compared with the position of the reference cracking pattern. A threshold maximum distance of about 2mm is imposed to discriminate actual crack points from misleading detections due to noise or convergence errors. Upper and lower bounds for the detectable cracks opening are progressively reduced as long as the analysis proceeds backwards towards the first load cycles. This selection aims at filter out cracks openings without physical meaning that could bias the statistical analysis and significantly affect the final result. Although the adopted methodology allows following the evolution of each crack throughout the test, in this work we are more interested in a global characterisation of the crack scenario. Spacing between cracks and averaged (or maximum) cracks widths are the values of main interest. Their estimation is required in engineering practice according to the formulas provided by standard codes. These parameters have been derived from statistical analysis of results concerning several cracks locations evaluated at different time steps.

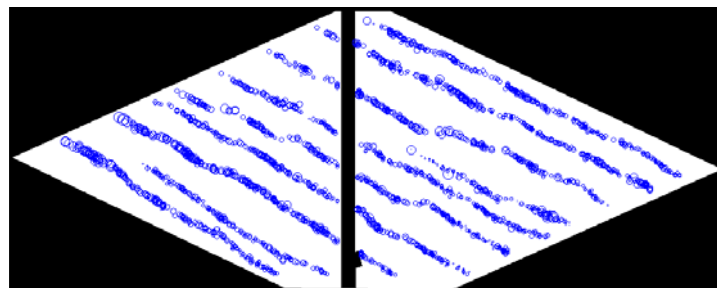


Figure 8. Reference crack pattern for the shear wall tested on mono-directional cyclic load.

4. AVERAGED CRACKS WIDTHS, SPACING AND ORIENTATION

The orientation of cracks and their spacing have been evaluated on the reference scenario when the crack pattern has been definitively established. For each detected crack, a regression line has been computed to ease the calculation of both crack orientation and spacing. Orientation has been defined as the angle between the regression line of the crack and the horizontal axis. Crack spacing has been obtained by subdividing each crack into a number of sections proportional to the crack's length and by averaging the distances between two consecutive cracks for all sections. Average values of both crack orientation and spacing at the last step of the mono-directional and bi-directional cyclic load histories

are collected in Table 4.1. Figures in brackets refer to a crack pattern limited to the very central area of the view under investigation (the six most central cracks), where the shear stress is supposed to be unaffected by bending.

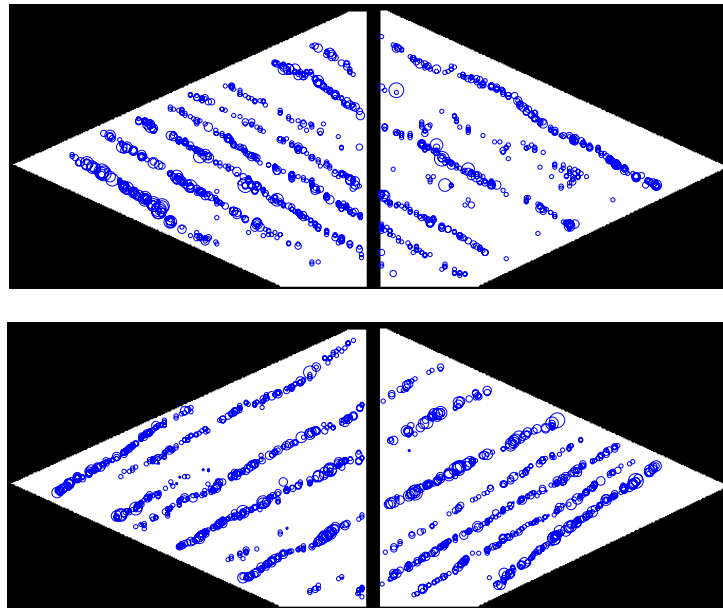


Figure 9. Reference crack patterns for the shear wall tested on bi-directional cyclic load: cracks widths for force F_1 applied towards the left-side (top) and for force F_2 applied towards the right-side (bottom).

No significant differences are detected for the orientation values between the two types of cycling load. On the contrary, a remarkable gap is observed in terms of cracks spacing. Moreover, equivalent results (for spacing and orientation) are obtained for each loading direction in the case of bi-directional cyclic load, i.e. left-side and right-side push. The average crack spacing has been compared with the prediction of Eurocode 2 where the cracks orientation is assumed equal to that measured by DIC, i.e. 28° . As suggested by Model Code 2010, a factor $2/3$ is adopted to estimate the required average value from the calculated maximal spacing. The obtained result is 133mm, which proves that Eurocode 2 over-estimates crack spacing compared to both types of cyclic load.

Table 4.1. Averaged crack parameters evaluated at the last loading step: $F = 4200\text{kN}$

	Averaged orientation [$^\circ$]	Averaged spacing [mm]	Averaged width [mm]
Mono-directional cyclic load (left-side push)	27,7 (26,6)	96,0 (94,0)	0,122 (0,121)
Bi-directional cyclic load (left-side push)	29,7 (28,8)	73,4 (77,7)	0,101 (0,088)
Bi-directional cyclic load (right-side push)	29,7 (27,7)	70,5 (78,8)	0,119 (0,121)

Evaluation of the crack widths has been furthermore analysed. For each step of the loading history, cracks of the reference patterns have been detected following the *modus operandi* described in the previous paragraph. All the points belonging to a crack have been selected (see Fig. 8-9) and their distribution of crack widths is supposed to be representative of the selected area of the shear wall (centre area). The mean value of the cracks widths obtained at the highest load step for the mono-directional and bi-directional loading tests is given in the last column of Table 4.1. Values in brackets refer to the crack pattern limited to the pure shear area (6 central cracks) of the mock-up. First of all, averaged width of cracks at the ultimate stage of the tests (4200kN) is comparable between mono and bi-directional cyclic load cases. However, in the case of bi-directional cyclic loading, a slight difference between the two sets of cracks (push right and push left) is observed, which is even more pronounced if the analysis is focused on the central area. The evolution of the cracks widths during the mono-directional cyclic load test is plotted in Fig. 10a. Blue lines refer to the loading steps, while red

lines refer to the unloading step. As a consequence, red lines give the residual opening at the end of unloading stage, when the applied force returns to 0 and cracks re-close. The mean values are plotted by solid lines. The spread of cracks width distribution for each load step is represented by a vertical dashed line, whose length is the double of the standard deviation. In the same figure, the percentage of opened cracks with reference to the final number of detections is plotted by a green solid line.

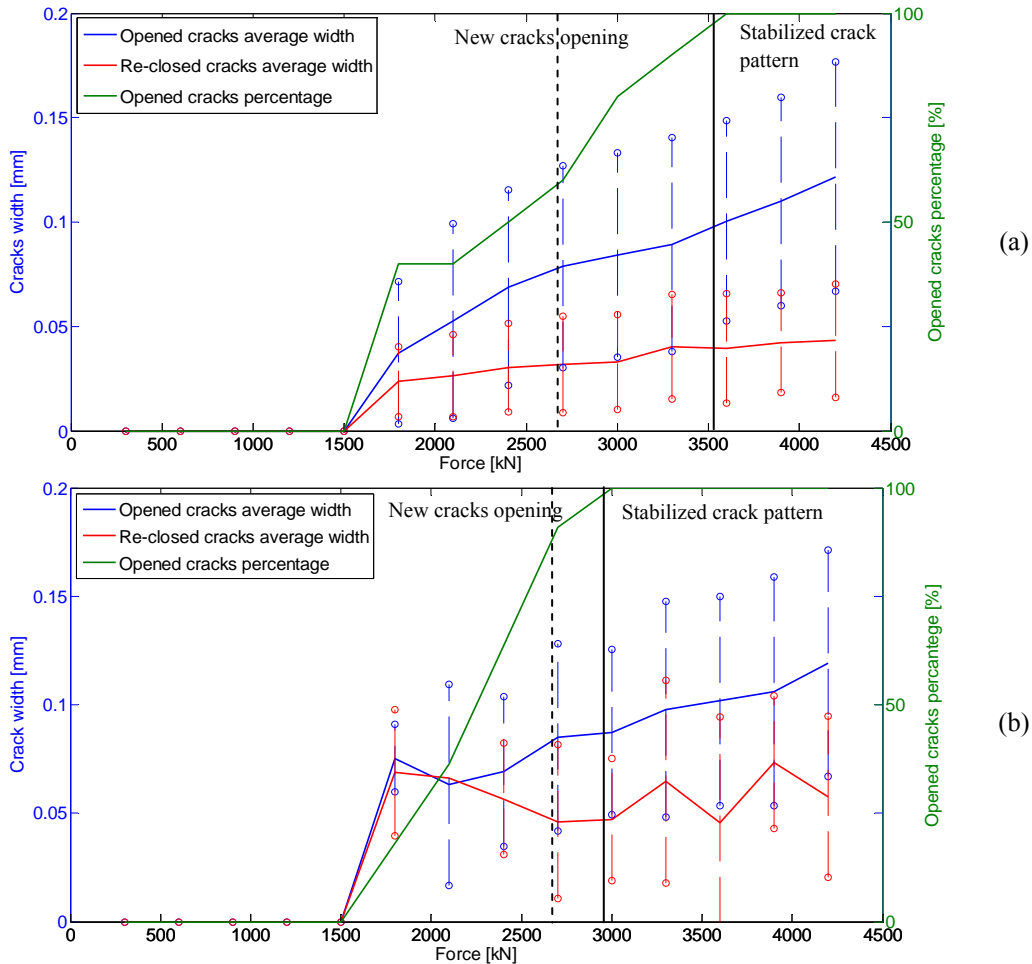


Figure 10. Evolution of the average cracks opening - mono-directional cyclic load test (a) and bi-directional cyclic load test (b): blue lines refer to loading steps and red lines to unloading steps.

As cracks cannot be measured under $30\mu\text{m}$, first cracks detection occurred at $F = 1800\text{kN}$, which is in agreement with the visual survey (see Fig. 4a). As expected, cracks width increases monotonously with the test. The number of opened cracks increases up to 3600kN , where the cracks pattern is completely established. Therefore, this load step marks the end of the new cracks formation phase. The transition towards the stabilized cracks pattern, where regular cracks space can be observed, is highlighted in Fig. 10a by a vertical solid line. A slight increase of the residual cracks width is observed throughout the test at the unloading steps (red lines). At the end of the test, residual cracks widths reach about 30% of the maximum crack widths measured at the last load step. Similar trends have been obtained for the left and right-push of the bi-directional cyclic load case (see Fig. 10b). Colours and line styles have the same meaning as in Fig. 10a. First cracks occur at 1800kN . Afterwards, the stabilization of the cracks pattern is extended over a shorter lapse of load cycles (up to 3000kN) compared to the mono-directional case. The evolution of the residual cracks opening is more discontinuous due to the difficulties in the detection of re-closed cracks. The residual cracks width reaches a final value which is almost 50% of the width measured at maximum load step, pointing out a significant difference compared to the mono-directional loading case. A numerical analysis was carried out on a FE (Code_ASTER) model of the mock-up that implements the nonlinear macroscopic constitutive rule called GLRC-DM (see Rachidi et al., 2012, for more details). Only the mono-

directional cyclic load case was analysed at the $F = 3\text{MN}$ force level. The stresses $\sigma_{xx} = -3,083\text{MPa}$, $\sigma_{yy} = 0,353\text{MPa}$, $\tau_{xy} = -4,42\text{MPa}$ were obtained in an element of the central area of the wall. These results have been used to calculate the stress in the steel bars and concrete ties according to the cracked membrane model (Kaufmann and Marti, 1998). The numerical analysis showed that the stresses in the horizontal reinforcement bars reach around 70% of the steel yield limit for $F = 3\text{MN}$. This allows setting the SLS limit to 2700kN (dashed vertical line in Fig. 10).

5. CONCLUSIONS

This work is part of an ongoing research program and aims at studying the capability of DIC to analyse the cracking of reinforced concrete walls subjected to shear cyclic loads. This measuring technique allows following the evolution of the whole crack pattern. Moreover, a large database is collected, which allows performing a rigorous statistical analysis. The comparison between the mono and bi-directional cyclic loads shows a substantial agreement in terms of average crack orientation and width. However, cracks spacing is larger in the mono-directional case. The cracks spacing formula of Eurocode 2 does not allow distinction between mono- and bi-directional cases. Moreover, the calculated value of the average spacing is larger than the one obtained from measurements. The average crack width increases monotonically during the test, while the spread of its distribution gives a useful indication about the stabilisation of the crack pattern. The latter is reached after the SLS, which has been set at 2700kN by a FE-based calculation. Cracks' re-closing is not complete because of the occurrence of irreversible strains. Cracks width has been seen to reach higher values at the ultimate stage for the bi-directional cyclic load than for mono-directional case.

ACKNOWLEDGEMENT

The investigation and results reported herein are supported by the French National Programme CEOS.fr (Study and design of specific structures in relation to cracking and shrinkage) sponsored by the French minister in charge of sustainable development (MEEDDM-DRI). The authors acknowledge the precious work done by A. Delaplace and C. Rouzaud in the acquisition of the digital images and the development of the DIC.

REFERENCES

- Kaufmann, W. and Marti, P. (1998). Structural concrete : Cracked membrane model. *Journal of Structural Engineering*, **124**:12,1467-1475.
- Pimentel, M., Brühwiler, E. and Figueiras, J. (2010). Extended cracked membrane model for the analysis of rc panels. *Engineering Structures*, **32**,1964-1975.
- Polak, M. A. and Vecchio, F. J. (1993). Nonlinear analysis of reinforced-concrete shells. *Journal of Structural Engineering*, **119**:12,3439-3462.
- CEB - FIP. Model Code 1990.
- FIB. Model Code 2010 - First draft, volume 2.
- Comité Européen de Normalisation. (2005). Eurocode 2. Calcul des structures en béton - Partie 1.1 : règles générales et règles pour les bâtiments.
- IREX. (2008). Programme National CEOS.FR - Programme Général.
- Rivillon, P. and Gabs, A. (2011). Projet National de Recherche CEOS, Axe 2 - Expérimentations, Rapport n°EEM 09 26023877-C. Technical Report, CSTB (in French).
- Demilecamps, L. et al. (2010). Reliable Shrinkage and Crack Design: Ceos.fr French National Research Program, Experimental Aspects. *3rd fib International Congress*.
- Sutton, M. A., Wolters, W. J., Peters, W. H., Ranson, W. F. and McNeill, S. R. (1983). Determination of Displacements Using an Improved Digital Correlation Method. *Im. Vis.Comp.* **1**, 133-139.
- Hild, F., Raka, B., Baudequin, M., Roux, S., Cantelaube, F. (2002). Multiscale displacement field measurements of compressed mineral-wool samples by digital image correlation. *Applied Optics*, 41:6815-6828.
- Rouzaud, C. (2011). Traitement de la mesure par analyse d'image et étude statistique de la fissuration de voiles en béton armé. Master 2 Recherche Report (in French), ENS Cachan and IOSIS Industries, Paris.
- Rachidi, M., Bisch, P., Erlicher, S. (2012). Numerical Modeling Cracks distance and opening in reinforced concrete membranes: codes predictions vs. experimental measurements. *International Conference on Numerical Modeling Strategies for Sustainable Concrete Structures*.